JCI The Journal of Clinical Investigation

Functionally identifiable apoptosis-insensitive subpopulations determine chemoresistance in acute myeloid leukemia

Patrick D. Bhola, Brenton G. Mar, R. Coleman Lindsley, Jeremy A. Ryan, Leah J. Hogdal, Thanh Trang Vo, Daniel J. DeAngelo, Ilene Galinsky, Benjamin L. Ebert, Anthony Letai

J Clin Invest. 2016;126(10):3827-3836. https://doi.org/10.1172/JCI82908.

Research Article **Hematology**

Upfront resistance to chemotherapy and relapse following remission are critical problems in leukemia that are generally attributed to subpopulations of chemoresistant tumor cells. There are, however, limited means for prospectively identifying these subpopulations, which hinders an understanding of therapeutic resistance. BH3 profiling is a functional single-cell analysis using synthetic BCL-2 BH3 domain–like peptides that measures mitochondrial apoptotic sensitivity or "priming." Here, we observed that the extent of apoptotic priming is heterogeneous within multiple cancer cell lines and is not the result of experimental noise. Apoptotic priming was also heterogeneous in treatment-naive primary human acute myeloid leukemia (AML) myeloblasts, and this heterogeneity decreased in chemotherapy-treated AML patients. The priming of the most apoptosis-resistant tumor cells, rather than the median priming of the population, best predicted patient response to induction chemotherapy. For several patients, these poorly primed subpopulations of AML tumor cells were enriched for antiapoptotic proteins. Developing techniques to identify and understand these apoptosis-insensitive subpopulations of tumor cells may yield insights into clinical chemoresistance and potentially improve therapeutic outcomes in AML.

Functionally identifiable apoptosis-insensitive subpopulations determine chemoresistance in acute myeloid leukemia

Patrick D. Bhola,[1] Brenton G. Mar,[2] R. Coleman Lindsley,[1] Jeremy A. Ryan,[1] Leah J. Hogdal,[1] Thanh Trang Vo,[1] Daniel J. DeAngelo,[1] Ilene Galinsky,[1] Benjamin L. Ebert,[3] and Anthony Letai[1]

[1]Department of Medical Oncology, Dana-Farber Cancer Institute, Boston, Massachusetts, USA. [2]Department of Pediatric Oncology, Dana-Farber Cancer Institute, Harvard Medical School, Boston, Massachusetts, USA. [3]Department of Medicine, Division of Hematology, Brigham and Women's Hospital, Harvard Medical School, Boston, Massachusetts, USA.

Upfront resistance to chemotherapy and relapse following remission are critical problems in leukemia that are generally attributed to subpopulations of chemoresistant tumor cells. There are, however, limited means for prospectively identifying these subpopulations, which hinders an understanding of therapeutic resistance. BH3 profiling is a functional single-cell analysis using synthetic BCL-2 BH3 domain–like peptides that measures mitochondrial apoptotic sensitivity or "priming." Here, we observed that the extent of apoptotic priming is heterogeneous within multiple cancer cell lines and is not the result of experimental noise. Apoptotic priming was also heterogeneous in treatment-naive primary human acute myeloid leukemia (AML) myeloblasts, and this heterogeneity decreased in chemotherapy-treated AML patients. The priming of the most apoptosis-resistant tumor cells, rather than the median priming of the population, best predicted patient response to induction chemotherapy. For several patients, these poorly primed subpopulations of AML tumor cells were enriched for antiapoptotic proteins. Developing techniques to identify and understand these apoptosis-insensitive subpopulations of tumor cells may yield insights into clinical chemoresistance and potentially improve therapeutic outcomes in AML.

Introduction

While cytotoxic chemotherapy can occasionally cure hematologic cancers, a significant portion of patients only partially respond or relapse (1). Often these relapsed or persistent tumors are refractory to multiple chemotherapies (2, 3). A proposed mechanism of partial response and of chemorefractory relapse is the selection of preexisting chemoresistant cells from the pretreatment tumor (4, 5). This is proposed to include the persistence of cancer stem cells (6) and of tumor subpopulations that are resistant to chemotherapy due to genetic lesions (7–9) or nongenetic features (9–11). Conventional cytotoxic chemotherapy, including cytarabine and daunarubicin, which are mainstays of first-line treatment of acute myeloid leukemia (AML), induce mitochondrial-mediated apoptosis (12, 13). We therefore reasoned that resistance to chemotherapy may be dictated by subpopulations that are most insensitive to mitochondrial-mediated apoptosis.

Mitochondrial-mediated apoptosis is a form of programmed cell death that is utilized during development and activated in response to cell stress. It is regulated by the BCL-2 family of proteins, which are characterized by the presence of at least 1 of 4 BCL-2 homology domains (BH1–4) and are divided into pro- and antiapoptotic members (14). Proapoptotic proteins (BIM, BID, PUMA, BAD, HRK, NOXA) are characterized by the presence of the third BCL-2 homology domain (BH3). Using BH3 domains, proapoptotic proteins either directly activate effector proteins BAX and BAK or antagonize antiapoptotic members (BCL-XL, BCL-2, BCLW, MCL1) (14). Activated BAX and BAK oligomerize to induce mitochondrial outer membrane permeabilization (MOMP) (15). The onset of MOMP is an irreversible step resulting in the release of cytochrome *c* from the mitochondria, which in turn activates the caspase proteases (16). These proteases, along with released mitochondrial nucleases, effect the cleavage of DNA and proteins and tag the plasma membrane with "eat me" signals that provoke phagocytic engulfment.

Many cytotoxic chemotherapies and many novel targeted therapies induce cellular stresses that result in the activation of mitochondrial-mediated apoptosis. This includes chemotherapies such as cytarabine and daunarubicin, which are mainstays of first-line treatment of AML. Prior studies have observed nonstochastic intracell line heterogeneity in cytotoxic response to several chemotherapies in several cell lines (10, 11, 17). However, the prevalence, clinical impact, and mechanistic underpinning of mitochondrial apoptotic heterogeneity in primary human tumors are unclear. An obstacle to functional measurements of apoptotic heterogeneity in primary human tumors is the extended culture time required. Although novel approaches have been undertaken to infer the apoptotic state of cells based on gene expression, these models are still under refinement, are fitted to individual cell-drug combinations, and have not been applied generally to human tumors (18).

To measure apoptotic sensitivity in uncultured primary human tumors, we used BH3 profiling (19, 20). BH3 profiling measures

Authorship note: B.G. Mar and R.C. Lindsley contributed equally to this work.
Conflict of interest: The authors have declared that no conflict of interest exists.
Submitted: June 8, 2015; **Accepted:** July 28, 2016.
Reference information: *J Clin Invest*. 2016;126(10):3827–3836. doi:10.1172/JCI82908.

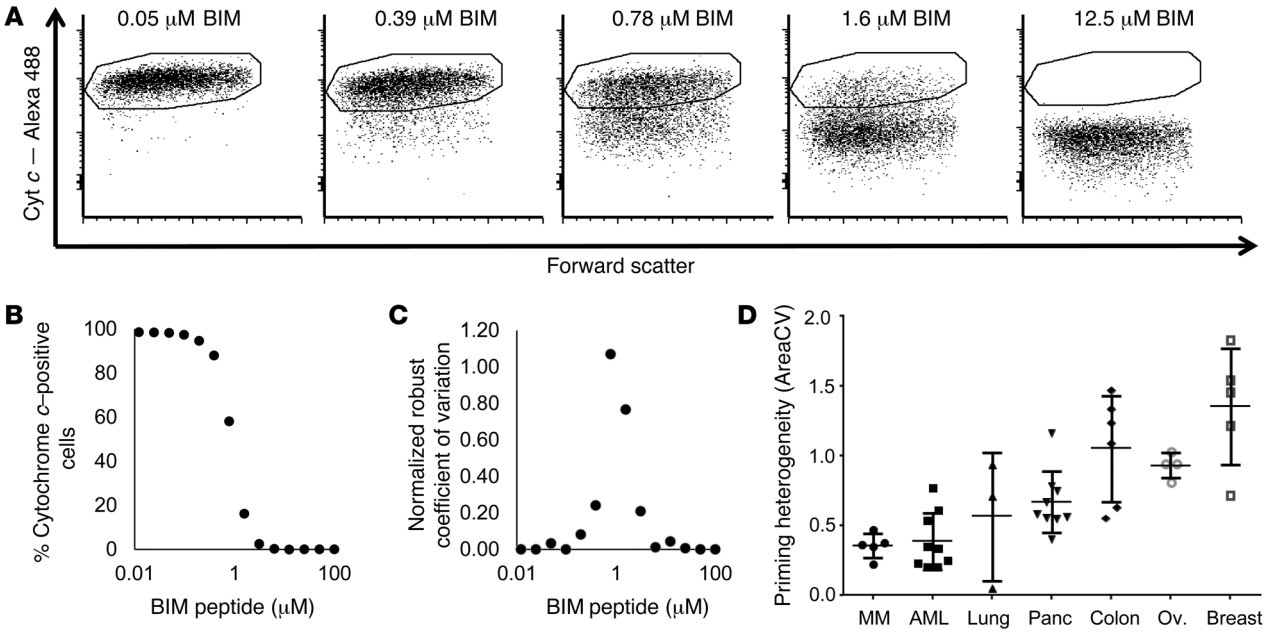

Figure 1. Cell-cell variability in mitochondrial priming is present in many cancer cell lines. (**A**) BH3 profile using increasing concentrations of the BIM peptide in the OCI-AML2 cell line. Scatter plots with cytochrome *c* immunofluorescence on the *y* axis and forward scatter on the *x* axis. Scatter plots are representative of 3 experiments. Cyt *c*, cytochrome *c*. (**B**) Quantification of average cytochrome *c* loss in the whole population. (**C**) Quantification of variability using the robust coefficient of variation — a measure of statistical dispersion. We calculate priming heterogeneity to be the area under this coefficient of variation curve. (**D**) Priming heterogeneity in cell lines from different malignancies. Panc, pancreas; Ov, ovary; MM, multiple myeloma. Error bars represent SD.

the proximity of cells to the mitochondrial apoptotic threshold — a phenotype we call mitochondrial apoptotic priming. Briefly, BH3 profiling entails permeabilizing plasma membranes of single cells to expose mitochondria to synthetic peptides modeled after the BH3 domains of the BCL-2 protein family. Upon exposure to the synthetic BH3 peptides, mitochondria in cells that are primed for apoptosis undergo MOMP as measured by loss of mitochondrial potential using dyes such as tetramethylrhodamine, ethyl ester (TMRE) or by loss of cytochrome *c* by immunofluorescence. Conversely, cells that are relatively unprimed for apoptosis do not undergo MOMP (21). In practice, one way we define apoptotic priming is by the concentration of synthetic BH3 peptide required to induce MOMP in a cell line or primary tumor.

Prior studies from our group demonstrated that mitochondrial priming of clinical specimens, measured as an aggregate or median across a distribution of cancer cells, is predictive of clinical parameters, such as patient response to cytotoxic chemotherapy and progression-free survival (12, 13). However, we have not previously examined whether the heterogeneity of priming across a distribution of cancer cells bears any clinical relevance. Here, we expand this earlier work in AML by performing single-cell measurements of BH3 profiles and show that primary AML tumor samples demonstrate cell-cell variability in apoptotic priming. We show that heterogeneity in apoptotic priming is greater in treatment-naive tumors compared with that in relapsed tumors. Furthermore, the proportion of unprimed subpopulations better predicts clinical response compared with bulk measurements of the tumor. Finally, using experimental approaches we believe to be novel, we identify subcellular features enriched in cells poorly primed for apoptosis.

Results

Heterogeneity in baseline mitochondrial apoptotic priming is present in multiple cancer cell lines. To develop tools for studying heterogeneity of apoptotic priming in primary human tumors, we first evaluated mitochondrial apoptotic priming heterogeneity in cancer cell lines. We saw no loss or partial loss of cytochrome *c* when OCI-AML2 AML cell lines were treated with low concentrations of the synthetic BIM peptide, while we saw complete loss of cytochrome *c* at high concentrations of the synthetic BIM peptide (Figure 1A). The onset of MOMP across the population is demonstrated by the progressive loss of cells from the cytochrome *c* high gate (Figure 1B). To measure the single-cell dispersion of apoptotic priming within a cell line, we measured the robust coefficient of variation at different BIM peptide concentrations (Supplemental Figure 1; supplemental material available online with this article; doi:10.1172/JCI82908DS1). Since baseline cytochrome *c* expression varies within a single cell line, we normalized the coefficients of variation within the population of cells to its value in the absence of synthetic BIM peptide (Supplemental Figure 1 and Figure 1C). Finally, to account for different average apoptotic priming in different cell lines, we calculated the area under the curve of the robust coefficient of variation normalized to average priming of that cell line to arrive at our measurement of priming heterogeneity. (Figure 1D and Supplemental Figure 1).

In applying this technique across several types of cancer cell lines, we found that apoptotic priming heterogeneity was not unique to AML cell lines (Figure 1D). Notably, solid tumor lines demonstrate larger variability compared with hematologic tumors. Furthermore, at high synthetic BIM BH3 peptide concentrations, several solid tumor cell lines and primary human ovarian

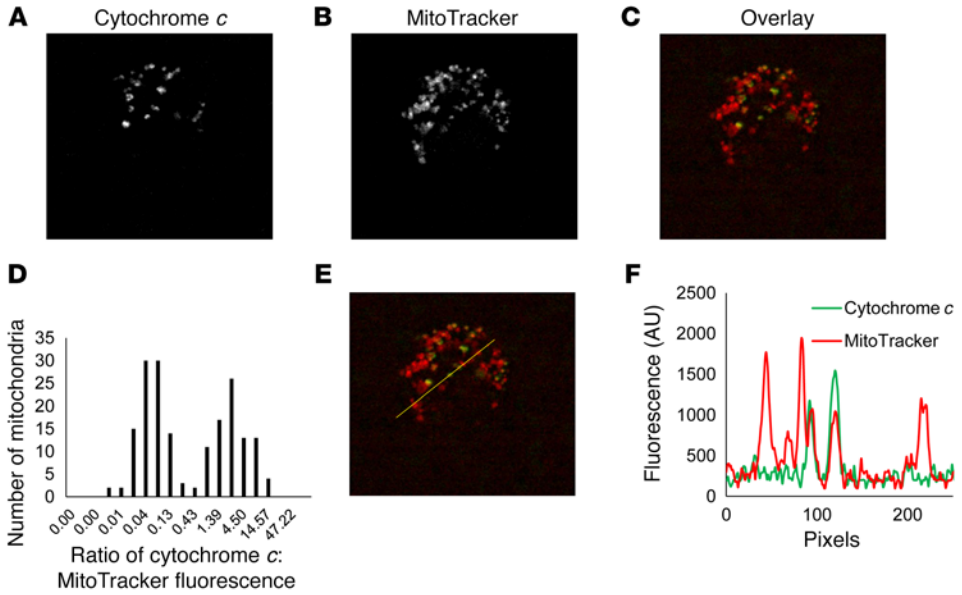

Figure 2. Subcellular heterogeneity in apoptotic priming in a cancer cell line. (**A**) Image of cytochrome *c* immunofluorescence in a Patu8902 cell after BH3 profiling with an intermediate level of cytochrome *c* retention. (**B**) Images of the MitoTracker mitochondrial dye, which stains all mitochondria, from the same cell as in **A**. (**C**) Overlay of cytochrome *c* (green) and MitoTracker (red) from the cell in **A** and **B**. (**D**) Histogram of cytochrome *c*/MitoTracker intensity showing a bimodal distribution of cytochrome *c* loss. Histogram represents an aggregate of 10 different cells. (**E**) Line scan through a cell in **C**. (**F**) Quantification of a line scan through the cell, demonstrating that mitochondria within the same cell are differentially primed for apoptosis. This line scan is representative of 7 different line scans. All images obtained with confocal microscopy. Original magnification, ×60.

ascites tumors contained subpopulations of cells with persistently intact mitochondria (Supplemental Figure 2). This is in contrast to the complete loss of cytochrome *c* that occurred in most AML cell lines. Overall, these results demonstrate that heterogeneity of baseline apoptotic priming is pervasive across different cancer cell lines and appears to vary by type of cancer cell line (1-way ANOVA; $P < 0.0001$).

Subcellular heterogeneity in mitochondrial priming. Prior studies indicate that the onset of MOMP is an all-or-nothing event within intact cells, resulting in a single-cell bimodal distribution of MOMP (22). However, during BH3 profiles, we did not see a bimodal distribution characteristic of an all-or-nothing event and, instead, observed a continuous distribution of cytochrome *c* loss (Figure 1). To interrogate this apparent discrepancy, we performed BH3 profiles on Patu8902 pancreatic cancer cells, then sorted and imaged single cells with intermediate levels of cytochrome *c* (Supplemental Figure 3A). We turned to an adherent cell line because of its superior imaging properties. Cells were stained prior to BH3 profiling with the MitoTracker Orange dye as a marker of mitochondria and were subsequently imaged using confocal microscopy (Figure 2, A–C). Complete Z-stacks were imaged for some cells (Supplemental Video 1). To quantify the loss of cytochrome *c* from individual mitochondria, we calculated the ratio of cytochrome *c* intensity to MitoTracker Orange intensity in single mitochondria across several cells and observed a bimodal distribution (Figure 2D). The bimodal loss of cytochrome *c* from single mitochondria across multiple cancer cells indicates an all-or-nothing release of cytochrome *c* from individual mitochondria during BH3 profiles.

The continuous distribution of BH3 profiles in a cell line combined with the all-or-nothing loss from individual mitochondria suggests that mitochondria in the same cell are differentially primed for apoptosis. To support this, we performed a line scan of fluorescence intensity across a single cell from Figure 2C and found that some mitochondria in the cell released cytochrome *c*, while others did not (Figure 2, E and F, and Supplemental Figure 3). Furthermore, histograms of cytochrome *c* intensity in mitochondria within the same cell also revealed a bimodal distribution (Supplemental Figure 3). To determine whether poor peptide access to mitochondria is responsible for differential cytochrome *c* release during the BH3-profiling assay, we directly measured the distribution of fluorescently conjugated peptides within the cell (Supplemental Figure 4) and found that peptide levels were uniformly distributed throughout the cell. These results suggest that, even within the same cell, individual mitochondria are differentially primed for apoptosis. Since we permeabilized the plasma membrane to perform the assay, it is possible that a diffusable factor had been lost that would coordinate MOMP across mitochondria in an intact cell. This could explain why prior studies have observed a biomodal distribution of cytochrome *c* release on the cellular level, while we saw a more continuous distribution.

Mitochondrial apoptotic priming heterogeneity reflects intrinsic biological heterogeneity and correlates with apoptotic heterogeneity. A critical concern about cell-to-cell heterogeneity phenotypes is whether the measured heterogeneity is intrinsically biological or a result of assay-based experimental noise. We reasoned that if genetic, epigenetic, or other biological differences are responsible for apoptotic priming heterogeneity of single whole cells observed in Figure 1, then sister cells should behave similarly. However, if apoptotic priming heterogeneity is solely a result of experimental noise in the BH3 profile measurement, we expect that sister cells would have different levels of apoptotic priming.

To measure apoptotic priming in sister cells, we tracked the lineage of adherent Patu8902 pancreatic cancer lines for up to 6 hours and subsequently performed BH3 profiles using time-lapse microscopy (Figure 3, A and B). Again, an adherent cell line was necessary for the imaging required for this experiment. The induction of MOMP was measured by the loss of mitochondrial membrane potential using the dye TMRE (Figure 3C). Figure 3B depicts a mother cell dividing into 2 daughter cells, and at time *t* = 0:00, cells were permeabilized and stained with the mitochondrial potential dye TMRE; the BIM BH3 peptide was then added. Over 1.5 hours, TMRE loss occurred in all cells, though at differ-

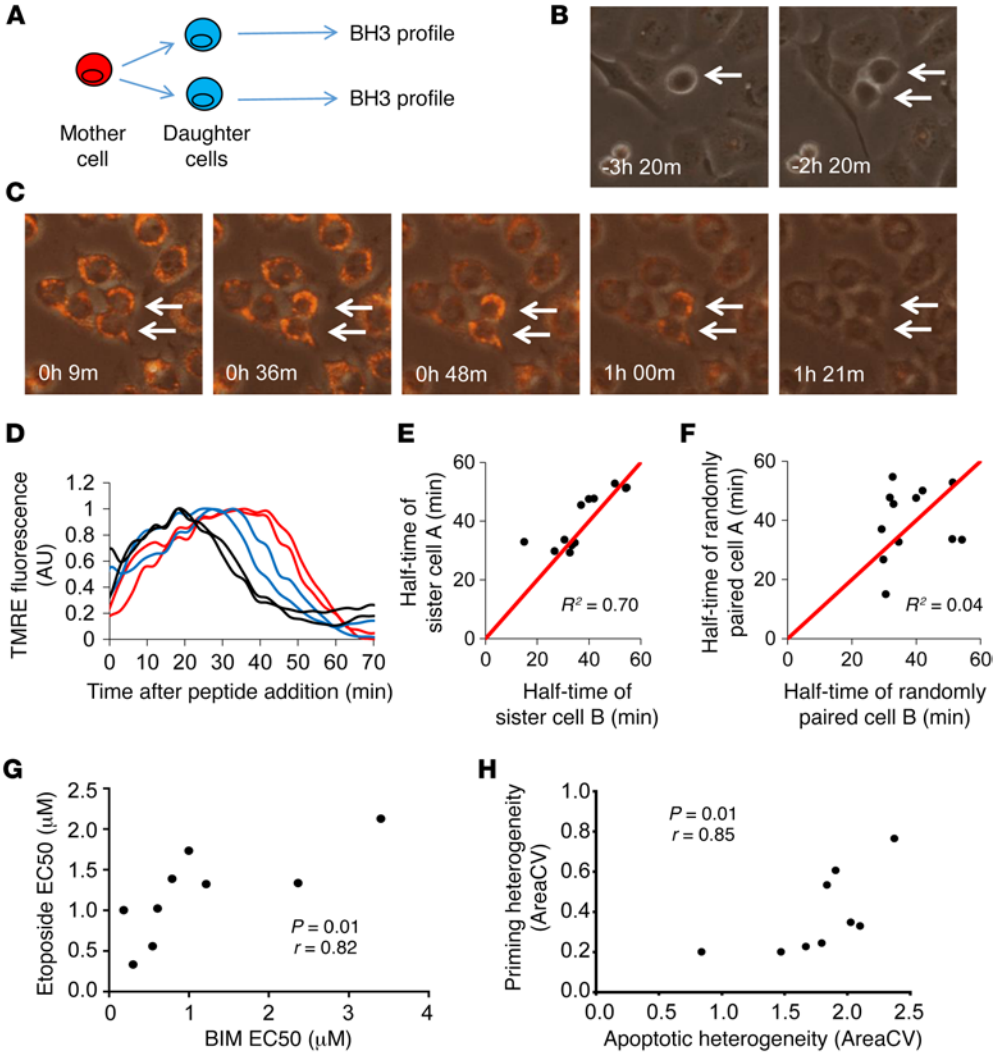

Figure 3. Mitochondrial priming heterogeneity reflects intrinsic and biological cell-to-cell differences. (**A**) Experimental overview. Cell lineages were tracked, and cells underwent BH3 profiling using time-lapse microscopy. (**B**) Images of a sister cell pair. (**C**) Images of BH3 profiling. Loss of TMRE indicates onset of MOMP. Images are representative of 3 different time lapses. All images obtained using wide-field microscopy. Original magnification, ×10. Arrows in **B** and **C** indicate a mother cell dividing into two sister cells (**D**) Quantification of TMRE loss in single cells. Sister cells are similarly colored. (**E**) Correlation of half-times of TMRE loss in sister cells. The red line represents an exact correlation between half-times (R^2 = 0.7). (**F**) Correlation of half-times of TMRE loss in randomly paired cells. The red line represents an exact correlation between half-times (R^2 = 0.04). (**G**) Correlation of apoptosis of AML cell lines in response to etoposide and baseline apoptotic priming in response to the synthetic BIM peptide (P = 0.01, Spearman r = 0.82). (**H**) Correlation between heterogeneity of apoptosis in response to etoposide (x axis) and apoptotic priming heterogeneity (y axis) (P = 0.01, Spearman r = 0.85).

ent times. Furthermore, the 2 sister cells appeared to undergo peptide-induced MOMP at similar times (Figure 3, B and C, and Supplemental Video 2). When the TMRE intensity from each cell is plotted as a function of time, sister cells show loss of TMRE at similar times (Figure 3D).

To assess sister cell similarity for multiple pairs, we fit the TMRE cells to a dose-response curve and calculated the half-time of TMRE loss. When the half-time of TMRE loss was quantified, we found that sister cell times correlated (Figure 3E) (R^2 = 0.70, P = 0.01), whereas randomly paired cells did not (Figure 3F) (R^2 = 0.04, P = 0.55). Sister cell similarity of BH3 profiles was also observed for SU86.86 pancreatic cells (Supplemental Figure 5). These results indicate that elements with at least short-term heritability, rather than experimental variability, are responsible for the variability of baseline apoptotic priming.

To assess the functional relevance of apoptotic priming heterogeneity, we sought to determine whether cell lines with high apoptotic priming heterogeneity also displayed high heterogeneity in their apoptotic cell death response to chemotherapy. We treated AML cancer cell lines for 48 hours with the DNA damage drug etoposide and calculated both the etoposide half-maximal effective concentration (EC_{50}) and heterogeneity in frank cell death at 48 hours (as measured by the robust coefficient of variation). Cell death was measured by FACS using loss of TMRE from single cells at 48 hours (Supplemental Figure 6). Similar to previous work from our lab, we found that average mitochondrial apoptotic priming correlated with frank cell death in AML cell lines (P = 0.01; Spearman r = 0.82, Figure 3G). Additionally, the heterogeneity of etoposide-induced apoptosis correlated with BH3 profiling heterogeneity (P = 0.01, Spearman r = 0.85, Figure 3H). This suggests that apoptotic heterogeneity in response to cytotoxic chemotherapy is in part determined by the pretreatment apoptotic state of mitochondria.

Overall priming and priming heterogeneity are reduced in myeloblasts from AML patients previously treated with chemotherapy. Given the demonstrated role of apoptotic priming in determining clinical chemotherapy response in AML (12), we hypothesized that chemotherapy treatment would select for less primed subpopulations. The result would be not only a reduction in priming, but also a reduction in priming heterogeneity. In fact, in an earlier study of 6 paired patient samples, we found that previously untreated AML samples were more primed relative to matched relapsed samples following chemotherapy response and relapse (12). No evaluation of heterogeneity was made in this study. Functional hetero-

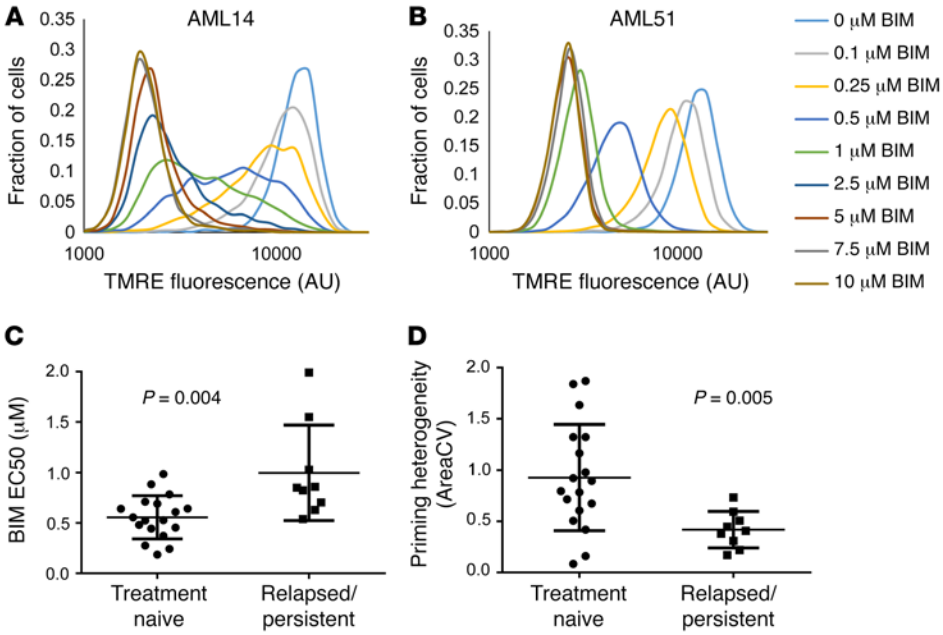

Figure 4. Treatment with cytotoxic chemotherapy decreases mitochondrial priming and decreases apoptotic heterogeneity in AML human samples. (**A**) Histogram of TMRE loss at different BIM peptide concentrations for relapsed patient AML14. (**B**) Histogram of TMRE loss at different BIM peptide concentrations for treatment of naive patient AML51. (**C**) Column correlation of BIM EC_{50} indicating that relapsed cells are less primed for apoptosis ($P = 0.004$, Mann-Whitney *U* test). (**D**) Column correlation of priming heterogeneity indicating that priming heterogeneity is decreased in relapsed tumors ($P = 0.005$, Mann-Whitney *U* test). Error bars represent SD.

geneity of mitochondrial apoptotic signaling in primary human tumors has been difficult to demonstrate owing to the extended culture time required for conventional functional apoptotic measurements. To investigate apoptotic heterogeneity in clinical samples without ex vivo culture, we applied BH3 profiling to primary human AML clinical samples. AML samples were isolated from patients, ficolled, and viably frozen. Prior studies from our lab indicate that freezing and thawing have minimal impact on apoptotic priming (12). Thawed primary AML samples were stained for CD45 and subjected to a flow cytometry–based BH3 profile. AML blasts were identified based on CD45 and side scatter plots as previously described (Supplemental Figure 7) (12).

In primary patient samples, we saw 2 general patterns of apoptotic priming in AML blasts: some tumors, such as AML14, demonstrated substantial heterogeneity in their BH3 profiles, as shown by the widening of the TMRE distributions after BIM BH3 peptide exposure. Other tumors, such as AML51, had more homogenous profiles (Figure 4, A and B, and Supplemental Figure 7). Similar to previous results from our lab, we found that untreated patients on average had myeloblasts that were more primed for apoptosis than those from chemotherapy-treated patients (Figure 4C) ($P = 0.004$). Furthermore, when we stratified clinical samples according to their treatment status, we found that treatment-naive samples had much more heterogeneous profiles compared with relapsed samples or posttreatment samples from patients with persistent tumors (Figure 4D) ($P = 0.005$). Treatment-naive AML patient tumors also had greater apoptotic priming heterogeneity compared with cultured AML cell lines (Supplemental Figure 8). While data in Figure 4 were obtained from a combination of bone marrow and peripheral blood samples, similar results were observed for samples derived only from bone marrow (Supplemental Figure 8 and Supplemental Table 1). These results demonstrate that persistent or relapsed tumors not only have decreased apoptotic priming as observed previously (12), but also have decreased heterogeneity of apoptotic priming. This supports the hypothesis that chemotherapy selects for poorly primed subpopulations present in the untreated leukemia patient.

We examined intracellular priming heterogeneity in primary AML tumors in a manner similar to the earlier analysis of intracellular priming heterogeneity in cancer cell lines (Figure 2). AML tumor cells were prestained with the MitoTracker Orange dye and were treated with an intermediate concentration of the synthetic BIM peptide. Cells were stained with a cytochrome *c* antibody and imaged using confocal microscopy. Images and quantitative line scans in cells indicate that, while some mitochondria retain cytochrome *c*, other mitochondria in the same cell release cytochrome *c* at intermediate concentrations of the BIM peptide (Supplemental Figure 9). Additionally, histograms of cytochrome *c* intensity in these cells indicate a biomodal distribution indicative of an all-or-nothing release of cytochrome *c* from individual mitochondria (Supplemental Figure 9). These results indicate that subcellular priming heterogeneity is also observed in primary tumors.

Unprimed apoptotic subpopulations best predict complete clinical response to chemotherapy. We next wanted to determine whether the least primed myeloblasts within a tumor were better predictors of clinical response compared with the median priming of a myeloblast population. If poorly primed subpopulations are selectively resistant to chemotherapy, then we would expect that the priming status of poorly primed outliers would affect clinical responses to chemotherapy. In the past, we have depended either on measurements aggregated over an entire population of cells or on the median of the distribution measured at a single concentration of BH3 peptide to predict clinical response. In order to better identify poorly primed subpopulations, we performed titrations of the BIM peptide in order to calculate different effective concentrations of BIM peptide required to induce MOMP in a fraction of the cells (Figure 5A). For example, the EC_{90} represents the amount of peptide required to induce MOMP in all but the 10% least primed cells. The EC_{50} measures the median mitochondrial apoptotic

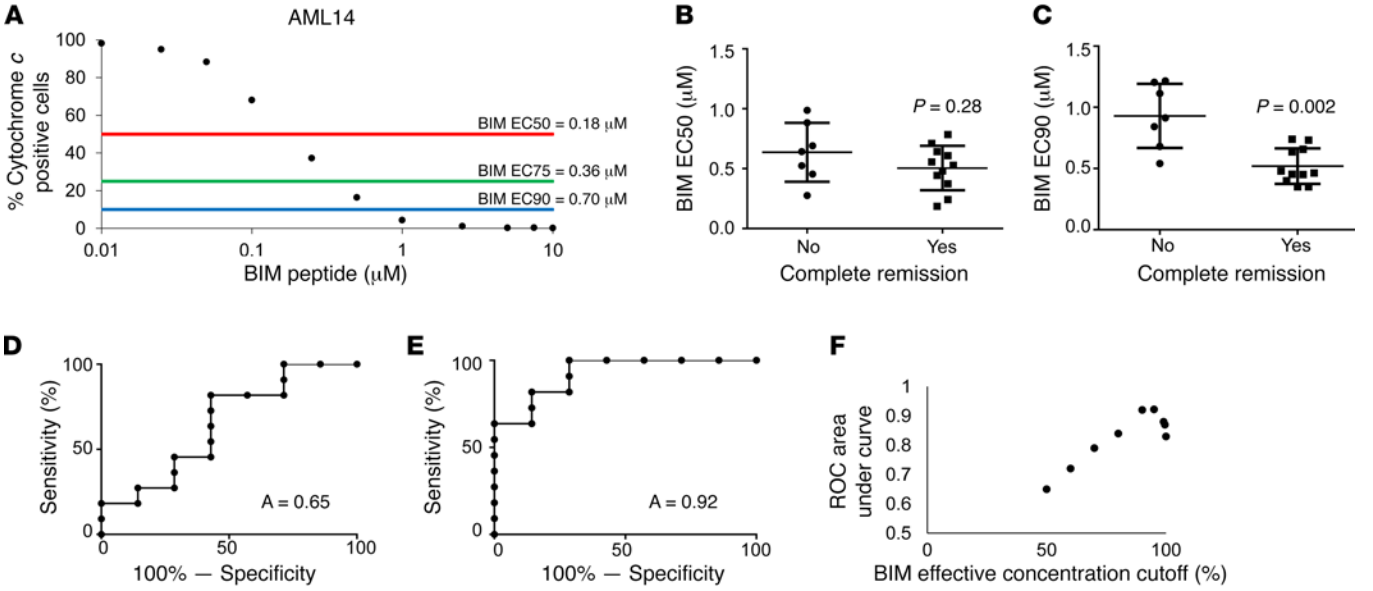

Figure 5. Poorly primed subpopulations predict complete remission in AML. (**A**) Dose-response curve of cytochrome *c* loss in BIM cells is used to identify the different effective concentrations of the BIM peptide. (**B**) Correlation of BIM EC_{50} and remission status of patients ($P = 0.28$, Mann-Whitney *U* test). (**C**) Correlation of BIM EC_{90} and remission status of patients ($P = 0.002$, Mann-Whitney *U* test). Error bars represent SD. (**D** and **E**) ROC for the BIM EC_{50} and BIM EC_{90} in predicting complete remission. (**F**) Area under curve from ROC analysis for different effective concentration cutoffs of the BIM peptide. The curve peaks at an effective concentration of 95%.

priming of the tumor. If the most unprimed cells are being selected by chemotherapy, we reasoned that characteristics of unprimed cells (EC_{90}) would better correlate with clinical response compared with average characteristics of the tumors (EC_{50}).

We considered how these metrics compare with patient outcomes in response to standard induction chemotherapy. While the EC_{50} values in treatment-naive patients failed to correlate with complete remissions ($P = 0.28$), the EC_{90} was a better predictor (Figure 5, B and C) ($P = 0.002$). Similar results were seen for other effective concentrations of the BIM peptide (Supplemental Figure 10). To determine how sensitive and specific unprimed subpopulations are at predicting complete remissions, we performed a receiver operating curve (ROC) analysis of the EC_{50} and the EC_{90} (Figure 5, D and E, and Supplemental Figure 10). We found that the EC_{90} was a more sensitive and specific indicator of complete remission ($A = 0.96$, $P = 0.001$) compared with the EC_{50} ($A = 0.65$, $P = 0.28$). We obtained a maximum ROC area using the EC_{95} ($A = 0.922$, $P = 0.002$) (Figure 5F). Finally, in comparing the EC_{90} value in treatment-naive and in posttreatment patients, we found that there is a significant difference in the EC_{90} between treatment-naive patients that undergo a complete response and posttreatment patients, but that there is no significant difference in the EC_{90} between treatment-naive patients that do not undergo a complete response and posttreatment patients (Supplemental Figure 10). Overall, these results suggest that, while there is some prognostic value to the EC_{50}, the EC_{90} provides even more sensitive and specific information of complete remission. These results suggest that poorly primed outliers are more important in determining clinical outcome than are the cells of average priming.

To assess the potential utility of measuring the EC_{90} of cytochrome *c* loss in response to the BIM BH3 peptide, we compared the EC_{90} to conventional predictors of clinical outcome in AML, such as age, blast percentage, and white blood cell count. We found no correlation between the EC_{90} and these conventional predictors of outcome (Supplemental Figure 11). Earlier studies indicated that patients with favorable cytogenetics were more primed for apoptosis as compared with patients that had intermediate cytogenetics (12). Here, while patients with favorable cytogenetics have a lower EC_{90} compared with patients with intermediate cytogenetics, this is not statistically significant ($P = 0.09$, Supplemental Figure 11). Of patients with intermediate cytogenetic prognosis, the BIM EC_{90} is lower in patients that undergo a complete response ($P = 0.01$, Supplemental Figure 11). These data indicate that the BIM EC_{90} offers distinct information compared with conventional predictors of outcome.

Prior genetic analysis of hematologic tumors indicates that clonal heterogeneity is associated with poor patient outcome (23). We sought to determine whether mitochondrial priming heterogeneity correlated with complete remission in treatment-naive patients using BH3 profiles of 20 treatment-naive patients (Supplemental Figure 11). When we correlated overall apoptotic heterogeneity with remission status, we did not find a correlation ($P = 0.41$). In sum, these results suggest that the presence of apoptotic priming heterogeneity in a single tumor is not sufficient to predict poor clinical response, but rather that the priming value of the most poorly primed cells best predicts a poor clinical outcome.

Enrichment of antiapoptotic proteins in unprimed cells. The BH3 profiling assay was developed as a way to make summary measurements of the apoptotic readiness of a cell. Its development was prompted largely by the difficulty in using abundance of individual proteins to make useful predictions about cellular apoptotic response following toxic stimuli. We wondered whether, in this clinical study, we could identify genes or gene products that could

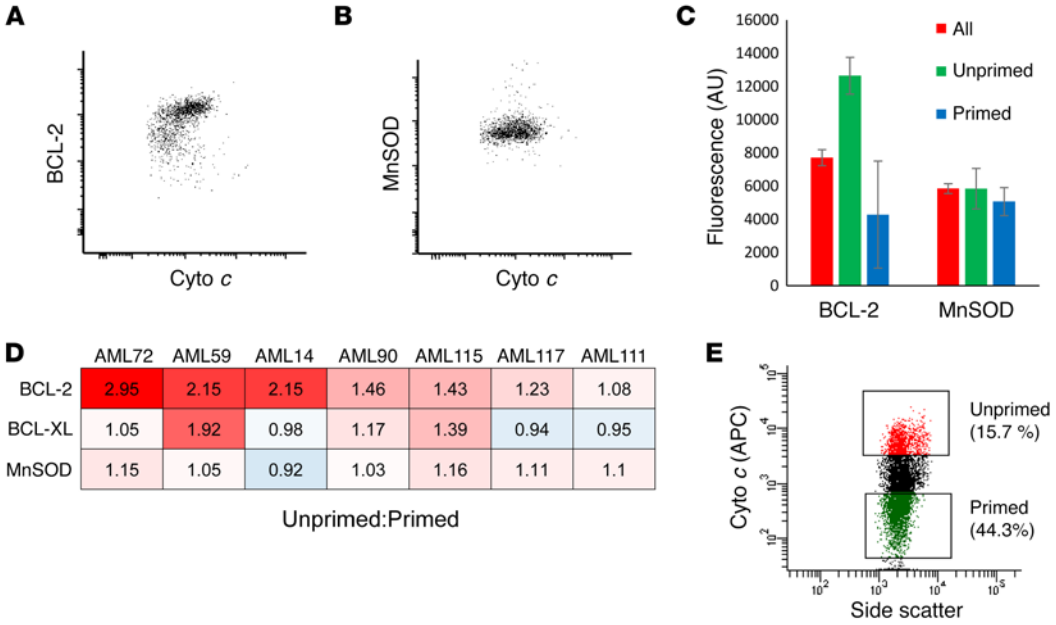

Figure 6. Differential immunofluorescence of BCL-2 proteins in unprimed cells. (**A**) Imunofluorescent staining of BCL-2 in cells after BH3 profiling of AML72 indicates that BCL-2 expression is low in primed cells and relatively higher in unprimed cells. (**B**) No difference in MnSOD staining in primed or unprimed cells. (**C**) Quantification of protein expression in the 10% most primed cells (primed), in the 10% least primed cells (unprimed), and in all cells (all). Error bars represent 95% CI of individual cells. (**D**) Quantification of the ratio of protein expression in unprimed/primed cells in different primary AML tumors for several apoptotic proteins. Red indicates that the protein is preferentially expressed in unprimed fractions. (**E**) Different populations of AML567 that were sorted and separately sequenced.

provide predictive information comparable to BH3 profiling. Given that the most unprimed cells best predict a complete clinical response, we sought to characterize proteins that were highly expressed in the most unprimed cells in primary AML samples. Although cytosolic proteins are lost during BH3 profiles, this assay itself does not result in widespread protease or nuclease activity as in most functional apoptosis assays, and many cellular features remain intact. Moreover, recent advances in the BH3 profile protocol facilitate the staining of intracellular proteins after BH3 profiles (24). We performed BH3 profiles of several AML samples at intermediate BIM peptide concentrations where there was dispersion of mitochondrial apoptotic priming. Cells were subsequently stained with antibodies against BCL-2 family proteins and cytochrome *c* to characterize apoptotic priming (Figure 6, A–C, and Supplemental Figure 12).

When AML72 was stained with cytochrome *c* and BCL-2 after a BH3 profile, a scatter plot of gated AML myeloblasts indicated that unprimed cells (higher cytochrome *c*) also had high levels of BCL-2 (Figure 6A). Importantly, the mitochondrial matrix protein manganese superoxide dismutase (MnSOD) showed no difference between primed and unprimed cells (Figure 6B). Notably, while BCL-2 is preferentially expressed in the unprimed apoptotic cells, high levels of BCL-2 do not uniquely predict single-cell apoptotic priming.

To determine differential protein expression in primed and unprimed subpopulations across multiple tumors, we quantified the immunofluorescence of proteins in the 10% most primed and 10% most unprimed cells, and compared the ratio of immunofluorescence. We found increased immunofluorescence of BCL-2 in unprimed cells, but no difference in MnSOD (Figure 6C). When we performed this across multiple tumors, in some instances, the BCL-2 and BCL-XL antiapoptotic proteins were highly expressed in the unprimed subpopulations, consistent with their actions as antiapoptotic proteins (Figure 6D and Supplemental Figure 12). In 2 of 7 tumors, we did not see a clear relationship between BCL-2 or BCL-XL and priming. This is not surprising, as mutations and potentially oncogenic pathways vary from patient to patient (25). Moreover, priming differences in these tumors may reflect differential protein levels of unmeasured proteins or other post-translational modifications to the measured proteins. Though it has been proposed that cells are more sensitive to apoptosis in different phases of the cell cycle, we found no difference in priming between cells in the G_1 phase and the S/G_2 phase (Supplemental Figure 12). In sum, while these results suggest that variable protein levels of BCL-2 or BCL-XL are in part responsible for altered apoptotic priming in some human tumor samples, the predictive information provided by these protein levels alone is limited compared with that of BH3 profiling.

Evaluations of mutations in primed and unprimed subpopulations. We finally sought to test whether there was a genetic signature that could usefully distinguish primed and unprimed subpopulations. Several studies indicate that treatment-naive AML tumors can consist of several genetically identifiable subclones (8) that have different functional properties (26). We BH3 profiled 3 AML primary samples and sorted the top 15% of unprimed blasts and the bottom 50% of primed blasts (Figure 6E and Supplemental Figure 13). Genomic DNA was extracted from each of these populations, and these were subjected to whole exome sequencing (>122× coverage). $CD3^+$ cells were used as a germline control, though AML driver mutations were found in the $CD3^+$ population (Supplemental Figure 13) as previously reported (27).

In 3 primary AML samples, we could find no significant differences in the variant allele fraction (VAF) between primed and unprimed subpopulations (Supplemental Table 2 and Supplemental Figure 13). This could result from sorting a large fraction of unprimed (~15%) and primed (~50%) cells or from a low depth of sequencing. Alternatively, in these patients, the differences between primed and unprimed subpopulations may not reflect genomic differences and instead may reflect epigenetic, gene-expression, or posttranslational differences. Our results suggest that it will be difficult in AML to find genetic signatures to substitute for BH3 profiling in identifying primed and unprimed populations.

Discussion

While many patients have been cured by conventional cytotoxic chemotherapy, most patients only partially respond to chemotherapy or fully respond, then relapse (1). Therefore, an important question in translational oncology is why some tumor cells within a single patient die in response to conventional cytotoxic chemotherapy while other cells survive (28). Our results suggest chemotherapy applies a selection pressure that culls the cells that are most primed for apoptosis, leaving behind a more homogeneous population of poorly primed AML cells. This culling of primed apoptotic cells explains why relapsed or persistent AML tumors are very often nonresponsive to a range of cytotoxic and targeted chemotherapies (2, 3). In fact, the presence of these unprimed subpopulations is so important that measurement of how primed they are is more predictive of clinical response than measurements made of the bulk of the tumor. The notion that a minority population in a tumor determines human clinical response is consistent with prior data in myelodysplastic syndrome–AML (MDS-AML) demonstrating that the detection of a poor prognosis mutation, even in a minor subclonal population, leads to poor clinical response (29). Ultimately, these observations demonstrate that reservoirs of poorly primed apoptotic cells within the larger tumor determine patient response in AML. Therefore, from a clinical standpoint, we propose that improved clinical outcomes will rely on identifying agents that, in combination with cytotoxic chemotherapy, increase apoptotic signaling in these poorly primed outliers.

A fundamental observation in this study is that individual mitochondria within cancer cell lines and primary AML tumor cells are differentially primed for apoptosis. The basis of this subcellular heterogeneity is unclear. Since proteins, especially the BCL-2 family (30), and lipids (31) are determinants of mitochondrial apoptotic signaling, it seems likely that heterogeneity in these factors is responsible. Alternatively, the age of individual mitochondria (32) or subcellular localization of mitochondria (33) may affect priming heterogeneity. Notably, the nuclear genome cannot be held responsible for subcellular mitochondrial priming heterogeneity as mitochondria, thus illustrating the limitations of considering genotype alone when analyzing factors responsible for sensitivity or resistance to chemotherapy in cancer. The functional importance of subcellular mitochondrial priming heterogeneity to the commitment of single-cell apoptosis is unresolved. Prior studies have found that within intact cells, all-or-nothing MOMP occurs as a wave across the cell, suggesting a feed-forward mechanism that amplifies MOMP from a few mitochondria into cell-wide MOMP (34, 35). This might suggest that the single most primed mitochondria in a cell determines the fate of the cell. However, cells can survive despite MOMP from one or a few mitochondria (36). These suggest that a critical number of primed mitochondria within a cell need to undergo MOMP to trigger all-or-nothing cell-wide MOMP.

Having identified a poorly primed subset of myeloblasts that disproportionately determine clinical outcome puts us in a better position to identify what molecular features distinguish these cells from the bulk of the tumor. We could not convincingly demonstrate a genetic basis for this difference. This might be possible in the future by the analysis of smaller subsets or by deeper sequencing. However, intratumoral apoptotic priming heterogeneity might not result from genetic factors and may instead be the result of cell-to-cell differences in epigenetics or proteins. Although we did see differences in single protein levels, these seemed of insufficient magnitude to explain the phenotypic priming differences alone. It seems likely that we are overlooking posttranslational modifications of BCL-2 proteins (37), the effects of combinations of BCL-2 proteins within single cells, or, indeed the participation of completely different proteins. Nonetheless, we do not think that it is a purely stochastic phenomenon based on stochastic differences in the expressions of key proteins. While stochastic protein expression differences have been suggested to affect response to chemotherapy, these differences are not stable, and the surviving cells rapidly resort to resemble the initial population (10, 11). Instead what we observe in clinical samples is a selection for a stably less primed and less heterogeneous population (12), inconsistent with purely stochastic effects.

We expect that a more comprehensive analysis of the genetic, epigenetic, intracellular, and cell-surface differences between primed and unprimed cells not only offers the potential to yield insights into why cells are resistant to chemotherapy, but may offer the potential to identify drug targets. By prospectively identifying and isolating unprimed subpopulations that are represented in relapse, we may better understand how to prospectively target them.

Methods

Cell culture and viability measurements. AML cell lines were cultured in RPMI with 10% FBS, penicillin, streptomycin, and L-glutamine. Solid tumor lines were either cultured in RPMI or in DMEM with 10% FBS, penicillin, streptomycin, and L-glutamine. All cell lines were obtained from the ATCC or as gifts from the Broad Institute Biologic Samples Platform (Cambridge, Massachusetts, USA). Apoptotic measurements of suspension were accomplished by treating cells with drugs for 48 hours, then adding in TMRE (50 nM) (Sigma-Aldrich) and Hoechst 33342 (10 nm) (Invitrogen) for 30 minutes, and measuring loss of membrane potential and loss of DNA integrity using a Fortessa flow cytometer (BD Bioscience). For more details, see Supplemental Methods.

Flow cytometry BH3 profiling. Flow cytometry–based BH3 profiling was performed as described earlier (24) using either cytochrome *c* or TMRE to measure MOMP. When using TMRE, cells were placed on ice to stop or slow depolarization after BH3 profiles were complete. Cancer cell lines were stained with Hoechst 33342 to eliminate dead cells from the analysis. Primary samples were BH3 profiled only once after being thawed. Primary AML specimens were stained with CD45-V450 (BD Biosciences) and Live Dead stains (Invitrogen). Costaining of cells with

cytochrome *c* and BCL-2 family proteins was performed simultaneously. Flow cytometry was performed on Fortessa cytometers or BD Canto cytometers at the Dana-Farber Cancer Institute Hematologic and Neoplasia Flow Cytometry Core. Data analysis and statistics were obtained from the Diva analysis program (BD Bioscience) or FCS Express. Image quality plots were produced using FCS Express. Antibodies used in this study were as follows: BCL-XL (2764S, Cell Signaling), anti-rabbit Alexa Fluor 555 (A21430, Life Technologies), CD45-V450 (642275, BD), cytochrome *c* Alexa Fluor 488/647 (560263, 558709, BD), BCL-2 PE (556537, BD), and MnSOD (S1450, Sigma-Aldrich).

Flow cytometry sorting experiments were performed using the FACSAria II (BD Biosciences). For sorting and sequencing experiments, cells were BH3 profiled, fixed with 1% EM grade paraformaldehyde, and stained according to earlier protocols (24). Genomic DNA was extracted after flow cytometry using QiaAMP DNA Mini Kit (QIAGEN). For more details, see *Extended experimental procedures*.

Microscopy. Live cell microscopy was performed on a Nikon inverted TE2000 microscope with a 10× objective. Cells were grown at 37°C with 5% CO_2 for 6 hours while undergoing live imaging, then washed and treated with BH3 profile buffers and peptides. Experiments were performed as biological duplicates with multiple imaging fields per experiment. High resolution of images of fixed cells after BH3 profiling and sorting was performed on a Yokogawa Spinning Disk Confocal Microscope with a 60× objective. All images were collected at the Dana-Farber Confocal Microscope Core. Images were analyzed in ImageJ (NIH) or with Metamorph. For more details see *Extended experimental procedures*.

Sequencing and variant calling. Genomic DNA was extracted after BH3 profiles using the Agilent DNA Kit. Genomic DNA was submitted for whole-exome sequencing (Exome Express – Broad Institute). Coverage ranged from 122× to 200×. Fastq files were aligned to the hg19 version of the human genome with BWA 0.6.2. Single-nucleotide and small insertion and deletion calling were performed with SAMtools 0.1.18 mpileup and Varscan 2.2.3. Annovar was used to annotate variants, including population allele frequency in 1000 Genomes (http://www.1000genomes.org/) and the Exome Sequencing Project (http://evs.gs.washington.edu/EVS/) and presence in COSMIC (http://cancer.sanger.ac.uk/cosmic). Variants were filtered out if they had less than 15 reads, were more than 50 bp outside of the defined exome capture baits, had excessive strand bias, or had an excessive number of calls in the local region. Variants that were known common stereotyped mutations in MDS and AML were prioritized in the calling.

Statistics. ROCs, column-based statistical tests, and curve fitting were performed in Prism 6.0. Spearman correlation coefficients were calculated. Mann-Whitney *U* column statistics were calculated. All *t* tests were 2 tailed, and *P* values of less than 0.05 were considered significant. All error bars represent SD unless otherwise indicated. Primary patient data are presented in Supplemental Table 1.

Study approval. Primary AML cells in this study were obtained with written informed consent from the Leukemia Group and Pasquerrelo Tissue Bank at the Dana-Farber Cancer Institute under IRB-approved protocol 01-206.

Author contributions

PDB and AL designed the study and wrote the manuscript. PDB performed experiments. DJD, IG, LJH, and TTV collected primary samples. LJH, TTV, and PDB processed primary samples and annotated patient data. JAR provided technical support. RCL, BGM, and BLE performed genomic analysis of the sorted BH3 profiles.

Acknowledgments

We thank John Daley, Suzan Lazo Kallanian, and the Dana-Farber Flow Cytometry Facility for assistance with flow cytometry, Lisa Cameron and the Dana-Farber Confocal Microscopy Core for assistance with microscopy, and Triona Ni Chonghaile for helpful discussions. Gabrielle's Angel Foundation for Cancer Research and grant P01 CA139980 (NIH) supported this research.

Address correspondence to: Anthony Letai, Dana-Farber Cancer Institute, 450 Brookline Avenue, Boston, Massachusetts 02215, USA. Phone: 617.582.7254; E-mail: Anthony_Letai@dfci.harvard.edu.

1. Burnett A, Wetzler M, Löwenberg B. Therapeutic advances in acute myeloid leukemia. *J Clin Oncol*. 2011;29(5):487–494.
2. Keating MJ, et al. Response to salvage therapy and survival after relapse in acute myelogenous leukemia. *J Clin Oncol*. 1989;7(8):1071–1080.
3. Kantarjian HM, Keating MJ, Walters RS, McCredie KB, Freireich EJ. The characteristics and outcome of patients with late relapse acute myelogenous leukemia. *J Clin Oncol*. 1988;6(2):232–238.
4. Nowell PC. The clonal evolution of tumor cell populations. *Science*. 1976;194(4260):23–28.
5. Greaves M, Maley CC. Clonal evolution in cancer. *Nature*. 2012;481(7381):306–313.
6. Nguyen LV, Vanner R, Dirks P, Eaves CJ. Cancer stem cells: an evolving concept. *Nat Rev Cancer*. 2012;12(2):133–143.
7. Mullighan CG, et al. Genomic analysis of the clonal origins of relapsed acute lymphoblastic leukemia. *Science*. 2008;322(5906):1377–1380.
8. Ding L, et al. Clonal evolution in relapsed acute myeloid leukaemia revealed by whole-genome sequencing. *Nature*. 2012;481(7382):506–510.
9. Hata AN, et al. Tumor cells can follow distinct evolutionary paths to become resistant to epidermal growth factor receptor inhibition. *Nat Med*. 2016;22(3):262–269.
10. Bhola PD, Simon SM. Determinism and divergence of apoptosis susceptibility in mammalian cells. *J Cell Sci*. 2009;122(Pt 23):4296–4302.
11. Spencer SL, Gaudet S, Albeck JG, Burke JM, Sorger PK. Non-genetic origins of cell-to-cell variability in TRAIL-induced apoptosis. *Nature*. 2009;459(7245):428–432.
12. Vo TT, et al. Relative mitochondrial priming of myeloblasts and normal HSCs determines chemotherapeutic success in AML. *Cell*. 2012;151(2):344–355.
13. Ni Chonghaile T, et al. Pretreatment mitochondrial priming correlates with clinical response to cytotoxic chemotherapy. *Science*. 2011;334(6059):1129–1133.
14. Czabotar PE, Lessene G, Strasser A, Adams JM. Control of apoptosis by the BCL-2 protein family: implications for physiology and therapy. *Nat Rev Mol Cell Biol*. 2014;15(1):49–63.
15. Wei MC, et al. Proapoptotic BAX and BAK: a requisite gateway to mitochondrial dysfunction and death. *Science*. 2001;292(5517):727–730.
16. Li P, et al. Cytochrome *c* and dATP-dependent formation of Apaf-1/caspase-9 complex initiates an apoptotic protease cascade. *Cell*. 1997;91(4):479–489.
17. Rehm M, Huber HJ, Hellwig CT, Anguissola S, Dussmann H, Prehn JH. Dynamics of outer mitochondrial membrane permeabilization during apoptosis. *Cell Death Differ*. 2009;16(4):613–623.
18. Lindner AU, et al. Systems analysis of BCL2 protein family interactions establishes a model to predict responses to chemotherapy. *Cancer Res*. 2013;73(2):519–528.
19. Certo M, et al. Mitochondria primed by death signals determine cellular addiction to antiapoptotic BCL-2 family members. *Cancer Cell*. 2006;9(5):351–365.
20. Ryan JA, Brunelle JK, Letai A. Heightened mitochondrial priming is the basis for apoptotic hypersensitivity of CD4+ CD8+ thymocytes. *Proc Natl Acad Sci U S A*. 2010;107(29):12895–12900.

21. Ryan J, Letai A. BH3 profiling in whole cells by fluorimeter or FACS. *Methods*. 2013;61(2):156–164.
22. Goldstein JC, Waterhouse NJ, Juin P, Evan GI, Green DR. The coordinate release of cytochrome *c* during apoptosis is rapid, complete and kinetically invariant. *Nat Cell Biol*. 2000;2(3):156–162.
23. Landau DA, et al. Evolution and impact of subclonal mutations in chronic lymphocytic leukemia. *Cell*. 2013;152(4):714–726.
24. Pan R, et al. Selective BCL-2 inhibition by ABT-199 causes on-target cell death in acute myeloid leukemia. *Cancer Discov*. 2014;4(3):362–375.
25. Papaemmanuil E, et al. Genomic Classification and Prognosis in Acute Myeloid Leukemia. *N Engl J Med*. 2016;374(23):2209–2221.
26. Klco JM, et al. Functional heterogeneity of genetically defined subclones in acute myeloid leukemia. *Cancer Cell*. 2014;25(3):379–392.
27. Shlush LI, et al. Identification of pre-leukaemic haematopoietic stem cells in acute leukaemia. *Nature*. 2014;506(7488):328–333.
28. Kleppe M, Levine RL. Tumor heterogeneity confounds and illuminates: assessing the implications. *Nat Med*. 2014;20(4):342–344.
29. Papaemmanuil E, et al. Clinical and biological implications of driver mutations in myelodysplastic syndromes. *Blood*. 2013;122(22):3616–3627; quiz 3699.
30. Letai AG. Diagnosing and exploiting cancer's addiction to blocks in apoptosis. *Nat Rev Cancer*. 2008;8(2):121–132.
31. Chipuk JE, et al. Sphingolipid metabolism cooperates with BAK and BAX to promote the mitochondrial pathway of apoptosis. *Cell*. 2012;148(5):988–1000.
32. Westermann B. Mitochondrial fusion and fission in cell life and death. *Nat Rev Mol Cell Biol*. 2010;11(12):872–884.
33. Rizzuto R, et al. Close contacts with the endoplasmic reticulum as determinants of mitochondrial Ca2+ responses. *Science*. 1998;280(5370):1763–1766.
34. Bhola PD, Mattheyses AL, Simon SM. Spatial and temporal dynamics of mitochondrial membrane permeability waves during apoptosis. *Biophys J*. 2009;97(8):2222–2231.
35. Lartigue L, et al. An intracellular wave of cytochrome *c* propagates and precedes Bax redistribution during apoptosis. *J Cell Sci*. 2008; 121(Pt 21):3515–3523.
36. Ichim G, et al. Limited mitochondrial permeabilization causes DNA damage and genomic instability in the absence of cell death. *Mol Cell*. 2015;57(5):860–872.
37. Kutuk O, Letai A. Regulation of Bcl-2 family proteins by posttranslational modifications. *Curr Mol Med*. 2008;8(2):102–118.